Journal of Applied Mechanical Engineering
ISSN: 2168-9873

Almasri et al., J Appl Mech Eng 2017, 6:5
DOI: 10.4172/2168-9873.1000286

Research Article Open Access

Analytical and Numerical Simulation of Dynamic Indentation for Different Indenter Shapes

Almasri AH[1], Safa'a Olimat[1] and Al Zubi M[2]*

[1]Department of Civil Engineering, Jordan University of Science and Technology, Irbid, Jordan
[2]Department of Mechanical Engineering, Tafial Technical University, Tafila, Jordan

Abstract

In this paper, an equation for calculating hardness under dynamic conditions is derived utilizing dislocation density definitions based on conservation of energy principle. In addition, finite element analysis of dynamic impact problems are carried out and compared to analytical solution to predict hardness behavior versus impact velocity for different indenter shapes. Indenter shapes considered in the research were spherical, cubical, and conical. Finite element results show reasonably good match with the analytical solution at low ranges of impact velocities, but diverge at higher values, which should be considered through different behaviors of deformation at such velocities.

Keywords: Simulation; Analytical; Dynamic hardness

Introduction

Contact between two solid bodies usually introduces the problem of localized stresses in these bodies. These stresses are usually given as a function of the normal contact force, the size of both bodies, and the modulus of elasticity (or generally material properties) of both bodies. Resistance of the material when subjected to these stresses is usually expressed as hardness, which is considered a material property.

Contact stress is found to be a function of material's type, indenter shape and loading conditions. It is found to be related to uniaxial stress flow at specific strains, represented by the well known Tabor equation [1]. Dynamic hardness can be obtained by impacting an indenter to the material surface. However, most of hardness and contact stresses formulations are based on static conditions, while many of real life problems are susceptible to impact loadings with high strain rates.

Many studies have been conducted to investigate contact stress problems for various conditions. One of the pioneers in this field was Tabor [1]; he studied the hardness using contact stress analysis, also he investigated the dynamic hardness which was defined as the resistance of the metal to local indentation produced by a rapidly moving indenter or dropped-ball. Contact stresses were estimated based on energy approach. Alternatively, dynamic hardness and the yield pressure were calculated based on rebound height measurements. The dynamic yield pressure was assumed constant during the impact, and ignored any increase in pressure during the early stage of impact due to dynamic effects. It is also assumed that elastic waves and change in temperature are neglected. The results showed that dynamic hardness results were always higher than the static hardness results. Ahn and Kwon [2] derived the true stress–true strain relationships of different grades of steel with different work-hardening exponents (0.1–0.3) from ball indentations. Four kinds of strain definitions in indentation were attempted: 0.2sin γ, 0.4hc/a, ln [2/ (1 + cos γ)], and 0.1tan γ, where, γ is the contact angle between the indenter and the specimen, hc is the depth of contact, and a is the radius of contact. The best strain definition was found to be 0.1tan γ. Moreover, the effect of piling-up or sinking-in were considered in determining the real contact between the indenter and the specimen from the indentation load–depth curve. The piling-up/sinking-in phenomena of various steels were found to be affected mainly by the work-hardening exponent. These phenomena markedly affected the absolute values of strain and stress in indentation by making the simple traditional relationship $P_m/\sigma_R \approx 3$ valid for the fully plastic regime. A practical method for measuring the hardness of metals at high strain rates (i.e. larger than $10^3\ S^{-1}$) has been developed and demonstrated by Clough et al. [3], using a dropped ball on cold-rolled 1018 plain carbon steel. One-dimensional rigid plastic metal is used. The dynamic hardness was obtained without the need for rebound energy corrections formulating the problem in terms of the indentation lateral dimensions. They noticed that a ballistic strain softening is unrecognized phenomenon occurred in projectile indentation of metals. It is related to the fact that the dynamic hardness obtained by this test is given in terms of the ball radius times the strain rate divided by the strain. The results indicate that there is a great enhancement strain hardening in irons and steels beyond a critical strain value. Nobre et al. [4] studied the surface resistance of a ductile steel to impact indentation by hard alumina balls with the help of pendulum machine. The deformation regime was found essentially to be elasto-plastic. Andrews et al. [5] investigated the impact of a sharp indenter at low impact velocities. By assuming that the indentation load variation in terms of depth under dynamic conditions has the same parabolic form as under static conditions, a one-dimensional model is developed and indention and rebounding motion from the target is described. It was found that for rate dependent materials, the relationship between the load and the depth in the impact problem is no longer parabolic and the model predictions cannot be applied in this case. Oka et al. [6] carried out analyses of plastic strain caused by a dynamic or quasi-static intrusion of a hard steel ball to study the plastic strain distributions and to search for triggers of erosion damage to materials around the indentation. For commercially pure aluminum, iron and grey cast iron, principal shearing strain distributions were obtained. They concluded that both the size and the form of the elastic-plastic boundary on the cross-sectional surface depend on the materials type and the intrusion processes. Sundararajan and Tirupataiah [7] studied the response of

***Corresponding author:** Al Zubi M, Assistant Professor, Department of Mechanical Engineering, Tafial Technical University, Tafila, Jordan, Tel: +962 3 225 0326; E-mail: malzuby@ttu.edu.jo

Received July 14, 2017; **Accepted** October 03, 2017; **Published** October 07, 2017

Citation: Almasri AH, Olimat S, Al Zubi M (2017) Analytical and Numerical Simulation of Dynamic Indentation for Different Indenter Shapes. J Appl Mech Eng 6: 286. doi: 10.4172/2168-9873.1000286

four metallic materials indented under conditions of static and dynamic indentation using spherical balls. Sundararajan and Tirupataiah [8] also analyzed the data from the companion paper within the framework of localization of plastic flow. They found that the dynamic hardness decreases beyond a critical strain, due to the onset of localization of plastic flow in the material being indented. Such localization is believed to be triggered by the stress flow decrease due to the temperature rise in the plastic zone. A composite expression for hardness under dynamic indentation conditions has been derived. Anton and Subhash [9] performed static and dynamic Vickers indentation on brittle materials to investigate the rate effects in hardness. An increase in hardness was observed in all the brittle materials under dynamic indentations compared to their measurements under static hardness. Stepanov and Zubov [10] presented essential results of experimental studies on dynamic hardness of a homogeneous rolled steel and titanium alloy. Komvopoulos and Yang [11] presented the analysis of a plane-strain of a dynamic indentation of an elastic-plastic multi-layered medium by a rigid cylinder using finite element method. Simulation results for the normal force, contact pressure distribution, subsurface stresses and evolution of plasticity in the multi-layered medium are presented as a function of the speed and the radius of the rigid indenter. The dynamic contact stresses between an axisymmetric projectile and an elastic half-space were obtained by Tsai [12] by solving three-dimensional equations of motion. These stresses are written as the sums of the Hertz contact stresses and wave-effect integrals. He found that for calculating the maximum radial surface stress at the maximum contact radius, the Hertz theory applies only when the contact time is longer than approximately 40 μsec. Tao et al. [13] presented a Three-dimensional finite element analysis of head and disk contact effects induced by impact in magnetic head disk interface (HDI). Elastic–plastic contact simulations are performed using finite element method. It was shown that finite element method can provide good simulation of the contact behavior resulting from the dynamic loading. Almasri and Voyiadjis [14] used two models to predict the strain rate dependency in hardness. A finite element analysis was carried out and compared with the two models proposed. Both models showed good agreement with the experimental results. Shinh-Chaun and Yu-Chang [15] studied the composite laminate and shell structures subjected to low velocity impact by finite element method. Numerical results show that greater stiffness, such as smaller curvature and clamped boundary conditions, leads to large contact force and smaller deflection. The impact response of the structure is proportional to the impact velocity.

Analytical Solution

Dynamic hardness is usually obtained by impacting an indenter to the material surface. Hardness H can be expressed in terms of dislocations density during deformations as follows [16-19]:

$$H = Zk\alpha Gb\sqrt{\rho_s + \rho_g} \tag{1}$$

where Z is the Taylor's factor, k is Tabor's factor, α is the statistical coefficient which accounts for the deviation from regular spatial arrangements of the dislocation population, G is the shear modulus, b is the magnitude of the Burger vector associated with dislocations, ρ_s is the statically stored dislocations (SSD) density, and ρ_g is the geometrically necessary dislocations (GND) density. Under dynamic condition, contact stresses and hardness values should depend on the velocity of the impact indenter according to kinetic energy principle. This kinetic energy of impact will be absorbed and transformed into material deformation represented by dislocations in case of metals. The kinetic energy E is expressed as:

$$E = \frac{1}{2}mV^2 \tag{2}$$

where m is the mass of the indenter, and V is the indenter impact velocity. It can be assumed that the kinetic energy of the indenter will be mainly stored in the material as strain energy or plastic deformation. However, the total strain energy per unit length of one dislocation E_d is given by [16]:

$$E_d = \frac{Gb^2}{4\eth} ln\left(\frac{R}{r_0}\right) \tag{3}$$

Where, R is the crystal radius, r_0 is the radius of dislocation. Taking an extremely small value for r_0, e.g. 0.1 nm and range values for R of 100mm to 1nm, the term $ln(R/r_0)$ will range from 2.3 to 20.7. For the purposes of simplifications, it is accepted in literature to let $ln(R/r_0)$ be considered approximately equals to 2 [16], and the strain energy will be:

$$E = \frac{Gb^2}{2\eth} \tag{4}$$

Assuming thermal changes are negligible; all of the indenter kinetic energy transforms mainly to strain energy in the impacted plate, so we have:

$$\frac{1}{2}mV^2 = E\rho_g v \tag{5}$$

Where v is the volume of deformation, which depends on the shape of the indenter, and can be found for spherical, cubical, and conical indenters to be:

$$v = \begin{cases} \frac{\pi}{3}D^2(3r - D) & \text{for spherical indenter} \\ a^2 D & \text{for cubical indenter} \\ \frac{\pi}{3}D^3 tan^2\theta & \text{for conical indenter} \end{cases} \tag{6}$$

Where D is the indentation depth, r is the sphere radius, a is the cube edge length, and θ is the cone angle. Substituting Eq. (6) and Eq. (4) in Eq. (5), a term for the geometrically necessary dislocations can be derived and substituted in Eq. (1) to obtain the following relations for hardness:

$$H = \begin{cases} Zk\alpha G\sqrt{b^2\rho_s + \frac{3mV^2}{GD^2(3r - D)}} & \text{for spherical indenter} \\ Zk\alpha G\sqrt{b^2\rho_s + \frac{\eth mV^2}{Ga^2 D}} & \text{for cubical indenter} \\ Zk\alpha G\sqrt{b^2\rho_s + \frac{3mV^2}{GD^3 tan^2\theta}} & \text{for conical indenter} \end{cases} \tag{7}$$

where Taylor's factor Z acts as an isotropic interpretation of the crystalline anisotropy at the continuum level with an average value of about 3.06 for metals, which was verified by other researchers (see for example [17]). The value of Tabor's factor k was found to be around 3 [18,19] while α is a statistical coefficient between 0.1 and 0.5 [20]. The empirical constant α accounts for the strength deviation from regular spatial arrangement of the SSD and GND populations, where SSDs is the stored dislocations generated by trapping each other in a random way, while GNDs is the stored dislocations that relieve the plastic deformation incompatibilities within the polycrystal caused by

non-uniform dislocation slip. More different values for the coefficient α can be found in literature, like 0.85 for SSDs [21] and 2.15 for GNDs [22]. In this paper, Z is taken to be 3.06, k is 3, α is 0.5, G is 80GPa, b is $2.5X10^{-10}$ m, and ρ_s is $10^{14}m^{-2}$. These values assure that the equation gives static hardness result when the second term under the square root vanishes (i.e. when impact velocity and indentation have small values).

Comparison with Finite Element Results

Dynamic explicit finite element method is used to simulate the impact process of indenter on steel plate. To allow for larger deformations, geometrical nonlinearity is used. In addition, bulk viscosity is used in the explicit analysis to prevent elements from collapsing under high velocity impacts. It also has a regularizing and enhancing effect on finite element mesh results where the need for very small finite elements disappears. Different three dimensional solid models are created for different indenters. The plate dimensions are 0.3x0.3x0.05 m, radii of spherical indenter are 0.01, 0.02, 0.03, 0.05 and 0.1m, cubical indenter edge length is 0.1m, and the conical indenter base radius is 0.1m and height is 0.1m with 45° angle. The boundary conditions are set to be fixed displacement at the bottom of the plate, and velocity boundary condition is assigned to the indenter part, which is simulated as a rigid body with no deformations. Cold rolled plain carbon steel (S1018) is assigned as the testing material, with density of 7800 Kg/m^3, Young's modulus of 200GPa, shear modulus of 80 GPa, yield strength of 400MPa, poisson's ratio of 0.3, with bilinear plastic behavior. The velocity and indentation depth are taken from the finite element results and plugged into Eq (7) in order to calculate the hardness, which is compared to the stress under indenter in the finite element model (as a representation for hardness) [22].

Numerical Results and Discussions

A typical stress distribution under an impacting spherical indenter moving with a velocity of 2m/s is shown in Figure 1, from which the indentation depth can be measured. Similar results for cubical and conical indenters are represented in Figures 2 and 3, simultaneously.

Hardness is directly proportioned to impact velocities and indenter masses, but inversely proportioned to indenter dimensions, which is clear in Eq.7. This is also illustrated in Figure 4. The equation shows slight nonlinear relation for hardness with impact velocities at low ranges of velocity, and more of a linear relation at higher ranges. All three indenters obtain close results for static hardness of about 950MPa at low velocities, but diverge while velocity increases. This might be attributed to the fact that every indenter will have different distribution of GNDs, which become higher with increasing velocity.

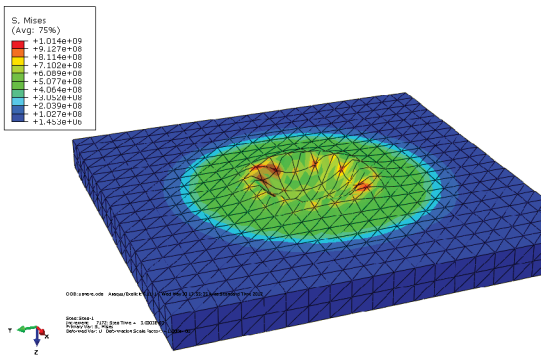

Figure 1: Pressure distribution under spherical indenter impacting a plate at a velocity of 2m/s (stresses are in Pa).

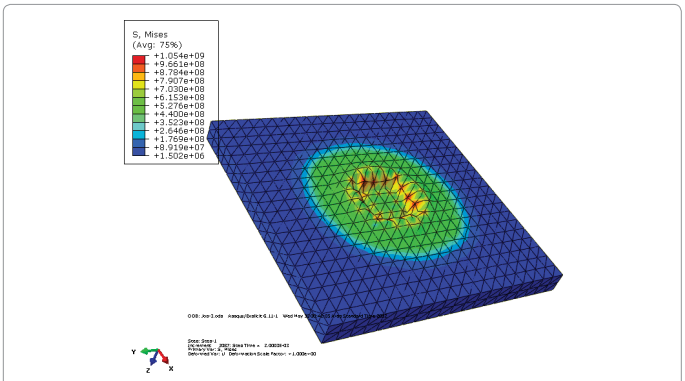

Figure 2: Pressure distribution under the cubical indenter impacting a plate at a velocity of 2m/s (stresses are in Pa).

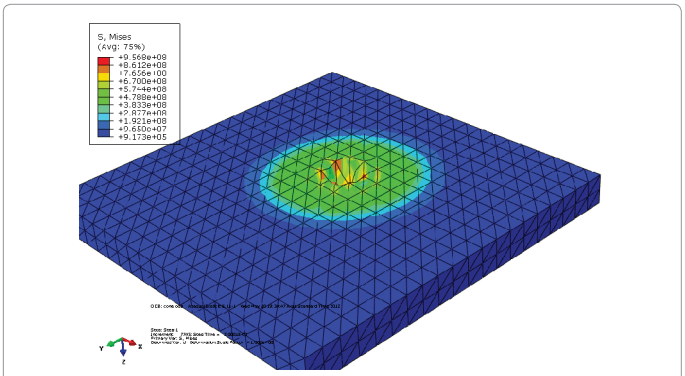

Figure 3: Pressure distribution under the conical indenter impacting a plate at a velocity of 1m/s (stresses are in Pa).

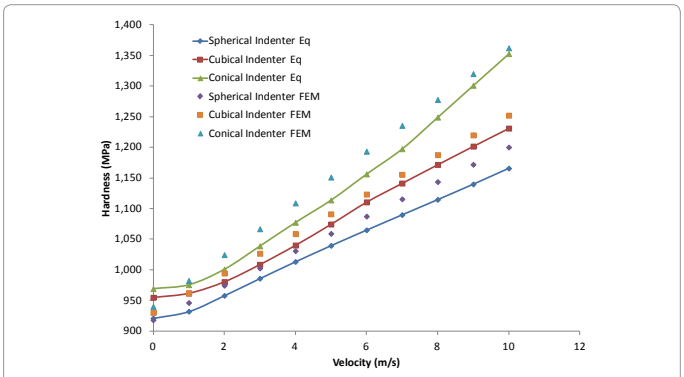

Figure 4: Hardness versus impact velocity for different indenters.

The FEM results of the average von mises stress under indenter are also represented in the figure to be compared with Eq (7) results. When the impact velocity is very small, no plastic indentation and deformation can be noticed in the elements, and hence a simulation for static indentation had to be run. Unlike the analytical solution, the FEM results show linear relation between hardness and impact velocity at all velocity values. Although there are good agreement between FEM and analytical solution, it can be seen that the FEM results are lower than the analytical solution at low impact velocities (below 2m/s), but become higher as the velocity increases.

Hardness is plotted versus spherical indenter mass and impact velocity in Figure 5. It shows that increasing indenter mass has a big, slightly nonlinear, effect on hardness-impact velocity relation, where

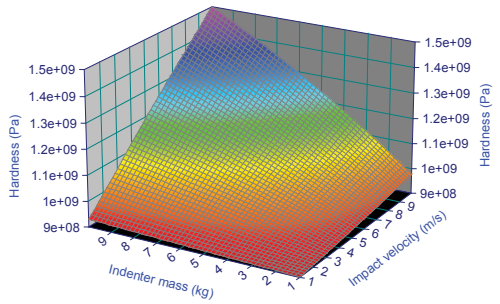

Figure 5: Hardness versus spherical indenter mass and impact velocity.

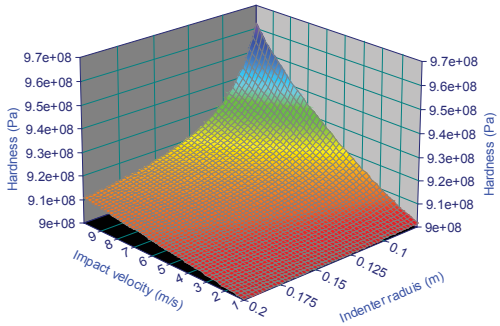

Figure 6: Hardness versus spherical indenter radius and impact velocity.

higher mass causes higher sensitivity of hardness versus impact velocity. Indenter radius (or indenter size) has inverse effect on hardness-impact velocity relation as illustrated in Figure 6. As the indenter size gets smaller, the hardness increases, which is expected since hardness is usually higher for smaller deformation scales.

Conclusions

In this study, dislocation densities were utilized to derive an equation for calculating hardness under dynamic conditions using conservation of energy principle. Finite element study of dynamic impact problems are also carried out and compared to analytical solution to predict hardness behavior against impact velocity for different indenter shapes. The relationship between the hardness and the impact velocity of indenters is found to have slight nonlinearity especially at small impact velocities, and similar behavior was obtained using the analytical model and the finite element solution, but with different divergences. Indenter mass and indenter size have been seen to have big effect (slightly nonlinear for the mass, and highly nonlinear for the size) on the relationship between the hardness and impact velocity. Analytical solution results were in good agreement with those of the finite element solution especially at low velocities. However, simulating impact at higher velocities needs incorporation of different deformation mechanisms such as strain localization and adiabatic deformation.

References

1. Tabor D (1950) The hardness of metals. Oxford: Clarendon Press.
2. Jeong-Hoon Ahn, Dongil Kwon (2001) Derivation of plastic stress–strain relationship from ball indentations: Examination of strain definition and pileup effect. J Mater Res 16: 3170-3178.
3. Roger Clough B, Stephen Webb C, Ronald Armstrong W (2003) Dynamic hardness measurements using a dropped ball: with application to 1018 steel. Mater Sci and Eng A360: 396-407.
4. Nobre JP, Dias AM, Gras R (1997) Resistance of a ductile steel surface to spherical normal impact indentation: use of a pendulum machine. Wear 211: 226-236.
5. Andrews EW, Giannakopoulos AE, Plisson E, Suresh S (2002) Analysis of the impact of a sharp indenter. Int J Solids and Structures 39: 281-295.
6. Oka YI, Matsumura M, Funaki H (1995) Measurements of plastic strain below an indentation and piling-up between two adjacent indentations. Wear 186: 50-55.
7. Sundararajan G, Tirupataiah Y (2006) The localization of plastic flow under dynamic indentation conditions: I. Experimental results. Acta Materialia 54: 565-575.
8. Sundararajan G, Tirupataiah Y (2006) The localization of plastic flow under dynamic indentation conditions: II. Analysis of results. Acta Materialia 54: 577-586.
9. Richard Anton J, Ghatu Subhash (2000) Dynamic vickers indentation of brittle materials. Wear 239: 27-35.
10. Stepanov G, Zubov V (2000) Dynamic hardness of high-strength steel and titanium alloy. J Phys 10: 647-651.
11. Komvopoulos K, Yang J (2004) Dynamic indentation of an elastic-plastic multi-layered medium by a rigid cylinder. ASME 126: 18-27.
12. Tsai YM (1971) Dynamic contact stresses produced by the impact of an axisymmetrical projectile of an elastic half-space. Int J Solids and Structures 7: 543-558.
13. Tao Q, Lee HP, Lim SP (2003) Contact analysis of impact in magnetic head disk interfaces. Tribology International 36: 49-56.
14. Almasri AH, Voyiadji's GZ (2007) Effect of strain rate on the dynamic hardness in metals. J of Eng Mater and Technol129: 505-512.
15. Shinh-Chaun H, Yu-Chang L (2004) The finite element analysis of composite laminates and shell structures subjected to low velocity. Composite Structures 66: 277-285.
16. Hull D, Bacon DJ (1975) Introduction to dislocations. 5th edn. Oxford: Linacre House, Jordan Hill.
17. Taylor GI (1938) Plastic strain in Metals. J Inst Met 62: 307-329.
18. Nix WD, Gao H (1998) Indentation size effects in crystalline materials: a law for strain gradient plasticity. J Mech Phys Solids 46: 411-425.
19. Kocks (1966) Computational mesomechanics of composites. England John Wiley & Sons Ltd.
20. Gilardi G, Sharf I (2002) Literature survey of contact dynamics modelling. Mechanism and Machine Theory 37: 1213-1239.
21. Kocks UF (1966) A statistical theory of flow stress and work hardening. Phill Mag 13: 541.
22. Busso EP, Meissonnier FT, O'Dowd NP (2000) Gradient-dependent deformation of two-phase single crystals. J Mech Phys Solids 48: 2333-2361.